

# Fabrication of Metal Nanoparticle Monolayers on Amphiphilic Poly(amido amine) Dendrimer Langmuir Films

Masaki Ujihara,<sup>†</sup> Koji Mitamura,<sup>†</sup> Naoya Torikai,<sup>‡</sup> and Toyoko Imae<sup>\*,†,§</sup>

Graduate School of Science, Nagoya University, Chikusa, Nagoya 464-8602, Japan, Neutron Science Laboratory (KENS), High Energy Accelerator Research Organization, Oho, Tsukuba 305-0801, Japan, and Research Center for Materials Science, Nagoya University, Chikusa, Nagoya 464-8602, Japan

Received November 27, 2005. In Final Form: December 29, 2005

A newly designed 1.5th generation poly(amido amine) dendrimer with an azacrown core, hexylene spacers, and octyl terminals was spread on gold nanoparticle (Au-NP) suspension. The surface pressure–area isothermal curves indicated that the molecular area of dendrimer on Au-NP suspension was significantly smaller than that on water, indicating the formation of dendrimer/Au-NP composites. The dendrimer Langmuir films on the Au-NP suspension were transferred to copper grids at various surface pressures and observed by transmission electron microscopy. The transferred films consisted of a fractal-like network of nanoparticles at low surface pressure and of a defect-rich monolayer of nanoparticles at high surface pressure. From these results, it was suggested that the dendrimers bind Au-NPs, and dendrimer/Au-NP composites formed networks or monolayers at the interface. From the intensity decrease of the Au plasmon band of Au-NP suspension after the formation of composite, it was estimated that some (~14) dendrimer molecules bind to one Au-NP. Furthermore, neutron reflectivity at the air/suspension interface and X-ray reflectivity of the film transferred on a silicon substrate revealed that the dendrimer molecules are localized on the upper-half surface of Au-NP. Metal affinity of azacrown, flexibility of hexylene spacer, and amphiphilicity of dendrimer with octyl terminals played important roles for the formation of dendrimer/Au-NP hybrid films. The present investigation proposed a new method to fabricate the self-assembled functional polymer/nanoparticle hybrid film.

## Introduction

Nanoparticles are attracting increasing attention as functional materials in the field of nanotechnology and as valuable materials on many applications<sup>1,2</sup> since they have different physical properties from bulk materials.<sup>3</sup> Recently, ordered structures fabricated by nanoparticles have been examined. Using an ordered template<sup>4–8</sup> or a shell on nanoparticle<sup>9–13</sup> is an effective method for preparing a film of ordered nanoparticles. While many systems are reported for fabricating such films, dendrimers are also used as shells for preparing nanoparticle-ordered films.<sup>14,15</sup> However, dendrimer templates for such a purpose are scarcely reported.

Since dendrimers are monodisperse in molecular weight and have many functional groups,<sup>16</sup> they are useful as building blocks for fabrication of nano-ordered structures such as self-assemblies,

liquid crystals, and ultrathin films.<sup>17</sup> Langmuir and Langmuir–Blodgett (LB) films<sup>18,19</sup> of amphiphilic dendrimers, dendrimer-adsorbed films,<sup>20</sup> dendrimer self-assembled monolayers (SAM),<sup>21–23</sup> and dendrimer-adsorbed thiol SAM<sup>24,25</sup> have been designed as ultrathin films. These dendrimer films might be ideal templates for the formation of nanoparticle films. Therefore, fabrication of dendrimer films and following dendrimer/nanoparticle hybrid films should be worthy of consideration.

Imae et al.<sup>26,27</sup> have investigated the structures of commercially available poly(amido amine) (PAMAM) dendrimers adsorbed onto solid surfaces and a thiol SAM. From these studies, it was concluded that terminal and interior groups of the dendrimer had respectively great influence on the interaction with the substrates. Recently, Imae's group has synthesized a novel PAMAM-type dendrimer (aza-C6-PAMAM dendrimer), which has an azacrown core and long repeating units (hexylene spacers),<sup>28</sup> different from commercial PAMAM dendrimers (ethylenediamine core, ethylene spacers). This aza-C6-PAMAM dendrimer was expected to be suitable for hybridization due to the adsorption of amine groups

\* To whom correspondence should be addressed. Phone: +81-52-789-5911. Fax: +81-52-789-5912. E-mail: imae@nano.chem.nagoya-u.ac.jp.

<sup>†</sup> Graduate School of Science, Nagoya University.

<sup>‡</sup> High Energy Accelerator Research Organization.

<sup>§</sup> Research Center for Materials Science, Nagoya University.

- (1) Bönnemann, H.; Richards, R. M. *Eur. J. Inorg. Chem.* **2001**, 2455.
- (2) Trindade, T.; O'Brien, P.; Pickett, N. L. *Chem. Mater.* **2001**, *13*, 3843.
- (3) Kamat, P. V. *J. Phys. Chem. B* **2002**, *106*, 7729.
- (4) Hornyak, G. L.; Kröll, M.; Pugin, R.; Sawitowski, T.; Schmid, G.; Bovin, J. O.; Karrson, G.; Hofmeister, H.; Hopfe, S. *Chem. Eur. J.* **1997**, *3*, 1951.
- (5) Lo, Y. M.; Price, R. R. *Colloids Surf., B* **2002**, *23*, 251.
- (6) Warner, M. G.; Hutchison, J. E. *Nat. Mater.* **2003**, *2*, 272.
- (7) Teranishi, T. *Comptes Rendus Chimie* **2003**, *6*, 979.
- (8) Costa, A. S.; Imae, T. *Trans. Mater. Res. Soc. Jpn.* **2004**, *29*, 3211.
- (9) Kiely, C. J.; Fink, J.; Brust, M.; Bethell, D.; Schiffrin, D. J. *Nature* **1998**, *396*, 444.
- (10) Kiely, C. J.; Fink, J.; Zheng, J. G.; Brust, M.; Bethell, D.; Schiffrin, D. J. *Adv. Mater.* **2000**, *12*, 640.
- (11) Manna, A.; Imae, T.; Iida, M.; Hisamatsu, N. *Langmuir* **2001**, *17*, 6000.
- (12) Manna, A.; Imae, T.; Yogo, T.; Aoi, K.; Okazaki, M. *J. Colloid Interface Sci.* **2002**, *256*, 297.
- (13) Manna, A.; Imae, T.; Aoi, K.; Okazaki, M. *Mol. Simul.* **2003**, *29*, 661.
- (14) Manna, A.; Imae, T.; Aoi, K.; Okada, M.; Yogo, T. *Chem. Mater.* **2001**, *13*, 1674.
- (15) Nakao, S.; Torigoe, K.; Kon-No, K. *J. Phys. Chem B* **2002**, *106*, 12097.
- (16) Tomalia, D. A. *Prog. Polym. Sci.* **2005**, *30*, 294.

(17) Smith, D. K.; Hirst, A. R.; Love, C. S.; Hardy, J. G.; Brignell, S. V.; Huang, B. *Prog. Polym. Sci.* **2005**, *30*, 220.

(18) Kajiyama, T.; Kojio, K.; Tanaka, K. *Adv. Colloid Interface Sci.* **2004**, *111*, 159.

(19) Hirano, C.; Imae, T.; Fujima, S.; Yanagimoto, Y.; Takaguchi, Y. *Langmuir* **2005**, *21*, 272.

(20) Tsukruk, V. V.; Rinderspacher, F.; Bliznyuk, V. N. *Langmuir* **1997**, *13*, 2171.

(21) Tokuhisa, H.; Zhao, M.; Baker, L. A.; Phan, V. T.; Dermody, D. L.; Garcia, M. E.; Peez, R. F.; Crooks, R. M.; Mayer, T. M. *J. Am. Chem. Soc.* **1998**, *120*, 4492.

(22) Chechik, V.; Crooks, R. M. *Langmuir* **1999**, *15*, 6364.

(23) Yamazaki, T.; Imae, T. *J. Nanosci. Nanotechnol.* **2005**, *5*, 1066.

(24) Nagaoka, H.; Imae, T. *Trans. Mater. Res. Soc. Jpn.* **2001**, *26*, 945.

(25) Nagaoka, H.; Imae, T. *Int. J. Non. Sci. Numer. Sim.* **2002**, *3*, 223.

(26) Imae, T.; Ito, M.; Aoi, K.; Tsutsumiuchi, K.; Noda, H.; Okada, M. *Colloids Surf., A* **2000**, *175*, 225.

(27) Ito, M.; Imae, T.; Aoi, K.; Tsutsumiuchi, K.; Noda, H.; Okada, M. *Langmuir* **2002**, *18*, 9757.

(28) Yemul, O.; Ujihara, M.; Imae, T. *Trans. Mater. Res. Soc. Jpn.* **2004**, *29*, 165.

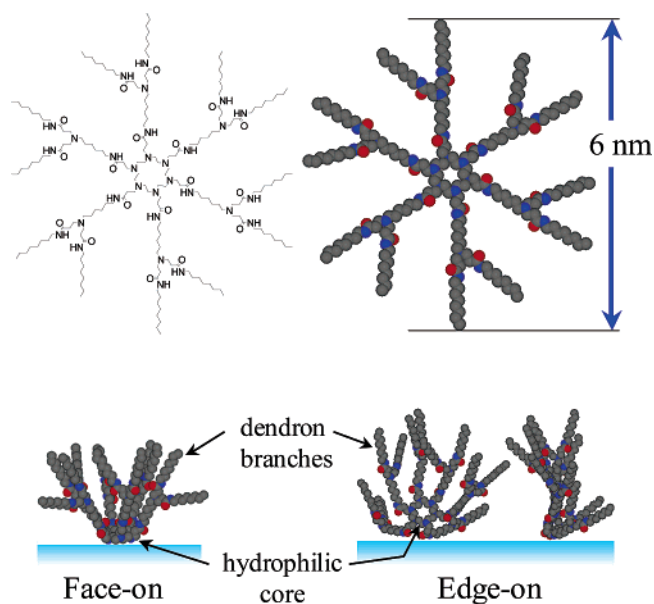


**Figure 1.** Chemical structure and conformations of G1.5 aza-C6-PAMAM dendrimer.

in azacrown and the flexibility of spacers. In a study of adsorption behaviors on a bare gold substrate and thiol SAMs immersed in solutions, the aza-C6-PAMAM dendrimers changed their conformation, and the peripheral amine groups were more dominant for adsorption than azacrown amines.<sup>29</sup> On the other hand, the azacrown in the dendrimer Langmuir film at air/suspension interface could interact with 3-mercaptopropionic acids that were protectors of silver nanoparticles in suspension.<sup>30</sup> However, such Langmuir films of methyl ester-terminated dendrimers easily collapsed at high surface pressures.

In the present study, terminal groups of the aza-C6-PAMAM dendrimer were substituted by a more hydrophobic moiety so that the long aliphatic groups in the periphery increase amphiphilicity of the dendrimer and contribute to form stable Langmuir films. Using this amphiphilic dendrimer, formation and structure of dendrimer/metal nanoparticle hybrid films were verified by surface pressure–area ( $\pi$ - $A$ ) isotherm, transmission electron microscopy (TEM), UV–vis absorption spectroscopy, neutron reflectometry, and X-ray reflectometry (XRR). Gold nanoparticles (Au-NP) protected with citric acid<sup>31</sup> were used. Then monolayers of metal nanoparticles should be fabricated on Langmuir films of amphiphilic PAMAM dendrimers. Thus, this study is useful for designing an ordered nanoparticle film on a functional polymer template.

### Experimental Section

**Chemicals.** Aza-C6-PAMAM dendrimer (1.5th generation (G1.5), methyl ester-terminated) was synthesized as previously reported.<sup>28</sup> Octylamine, NaAuCl<sub>4</sub> dihydrate, citric acid monohydrate, NaBH<sub>4</sub>, and CHCl<sub>3</sub> were purchased from Aldrich Co. or Tokyo Kasei Co. and used without further purification. The ultrapure H<sub>2</sub>O (resistivity of 18 M $\Omega$  cm and surface tension of 72.6 mN m<sup>-1</sup> at 25.0  $\pm$  0.5  $^{\circ}$ C) was obtained from a Milli-Q Labo ultrapure water system (Millipore Corp.). D<sub>2</sub>O (99.9%) was purchased from Cambridge Isotope laboratories, Inc. and used only for neutron reflectivity measurements.

**Synthesis of Octyl-Terminated G1.5 Aza-C6-PAMAM Dendrimer (Figure 1).** A total of 0.23 g (0.1 mmol) of G1.5 aza-C6-PAMAM

dendrimer was mixed with 0.52 g (4.0 mmol) of *n*-octylamine. The mixture was incubated at 40  $^{\circ}$ C for 4 days, and excess *n*-octylamine was removed by distillation in vacuo at 40  $^{\circ}$ C. The residue was dissolved in CHCl<sub>3</sub> and washed 3 times with water. The solvent was removed by evaporation, and yellowish oil was obtained (0.29 g, yield 83%).

**Synthesis of Gold Nanoparticles Protected by Citric Acid (Au-NP).** A total of 0.02 g (0.05 mmol) of NaAuCl<sub>4</sub> dihydrate and 0.01 g (0.05 mmol) of citric acid monohydrate were dissolved in 100 g of water. To this solution was added a freshly prepared aqueous NaBH<sub>4</sub> solution (100 g, 6.0 mM, 0  $^{\circ}$ C) at once with vigorous stirring. After it was mixed, the colorless solution turned orange immediately and vermilion within a few minutes. The suspension was kept under mild stirring at room temperature for 2 h and diluted with water to 1000 cm<sup>3</sup> (Au atom: 0.05 mM). This suspension was used as subphase on subsequent measurements. The obtained gold nanoparticles were 3.9  $\pm$  0.7 nm in diameter, which was determined from a TEM image.

**Measurements.** Measurements of the  $\pi$ - $A$  isotherm were carried out at 25  $^{\circ}$ C by using a Wilhelmy plate (accuracy:  $\pm$ 0.01 mN m<sup>-1</sup>) in a LB film deposition apparatus (trough size 323 mm  $\times$  50 mm, Nippon Laser & Electronics Laboratory). A CHCl<sub>3</sub> solution (30 mm<sup>3</sup>) of G1.5 dendrimer (0.1 mM) was spread on water or the Au-NP suspension subphase and kept for 1 h for solvent evaporation. The Langmuir film was compressed at a rate of 10 mm/min and was transferred by means of the Langmuir–Schaefer method (horizontal lifting method)<sup>32,33</sup> to a copper grid (Nissin EM300 mesh) covered with carbon film. TEM observation of the transferred film was performed using a Hitachi H-7000 instrument at an acceleration voltage of 100 kV.

G1.5 dendrimer (10<sup>-9</sup> mol) in CHCl<sub>3</sub> was spread on a Au-NP suspension (20 cm<sup>3</sup>) in a Petri dish (subphase surface area: 38 cm<sup>2</sup>), and the Petri dish was covered and left at rest. After the prescribed period (1 h and 24 h), the dish was recorded by photograph (digital camera), and the UV–vis absorption spectrum of the subphase was recorded with a Shimadzu UV 2200 spectrometer using a quartz cell (10 mm path). Furthermore, the LB film was also prepared from the Langmuir film by the Langmuir–Schaefer method and observed with TEM as described above.

Neutron reflectivity measurements were carried out on an ARISA (advanced reflectometer for interface and surface analysis) of the High Energy Accelerator Research Organization (KEK) in Tsukuba, Japan, equipped with a trough (370 mm  $\times$  120 mm). The operations of the ARISA and the trough were described elsewhere.<sup>34,35</sup> A CHCl<sub>3</sub> solution (200 mm<sup>3</sup>) of G1.5 dendrimer (0.1 mM) was spread on water or the Au-NP suspension subphase. After 1 h, the film was compressed at 12 mm/min until the surface pressure reached to 5 mN/m. Then, the neutron reflectivity was recorded with keeping 5 mN/m. The measurements were performed at a wave vector magnitude  $q$  ( $= 4\pi\sin\theta/\lambda$ ,  $\theta$ : incident angle,  $\lambda$ : wavelength) range of 0.08–2.3 nm<sup>-1</sup>. The data were analyzed by the program “mlayer” with 7% error of the  $q$  value.

X-ray reflectivities were measured on a Rigaku RINT 2500 instrument with an X-ray beam ( $\lambda = 0.154$  nm) from a Cu K $\alpha$  X-ray source (200 mA/40 kV), which was monochromized by a multilayered mirror. The divergence and receiving slits were respectively 0.05 and 0.1 cm in width. The sample stage was adjusted by a goniometer. The scan rate was 0.04 $^{\circ}$ /min, and the angle step was 0.001 $^{\circ}$ . The Langmuir film was prepared by using the same procedure as the measurement of  $\pi$ - $A$  isotherm (described above), and the surface pressure was kept at 10 mN/m for transferring the film onto a silicon substrate.

The neutron and X-ray reflection curves were analyzed by using an equation described elsewhere,<sup>36</sup> and the scattering length density

(32) Brown, J. J.; Porter, J. A.; Daghighian, C. P.; Gibson, U. J. *Langmuir* **2001**, *17*, 7966.

(33) Santhanam, V.; Liu, J.; Agarwal, R.; Andres, R. P. *Langmuir* **2003**, *19*, 7881.

(34) Torikai, N.; Furusaka, M.; Matsuoka, H.; Matsushita, Y.; Shibayama, M.; Takahara, A.; Takeda, M.; Tasaki, S.; Yamaoka, H. *Appl. Phys. A* **2002**, *74*, 264.

(35) Mitamura, K.; Takahashi, M.; Hamaguchi, S.; Imae, T.; Nakamura, T. *Trans. Mater. Res. Soc. Jpn.* **2004**, *29*, 255.

(36) Parratt, L. G. *Phys. Rev.* **1954**, *95*, 359.

(29) Ujihara, M.; Imae, T. *J. Colloid Interface Sci.* **2006**, *293*, 333.

(30) Ujihara, M.; Orbulescu, J.; Imae, T.; Leblanc R. M. *Langmuir* **2005**, *21*, 6846.

(31) Cumberland, S. L.; Strouse, G. F. *Langmuir* **2002**, *18*, 269.

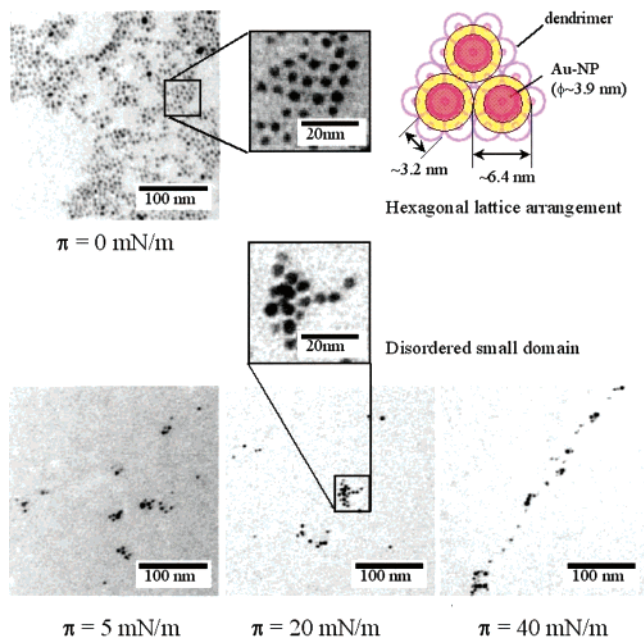


**Figure 2.** TEM images of Au-NPs adsorbed on the dendrimer LB films prepared at various surface pressures.

(SLD) or electron density, thickness, and roughness of each layer were calculated. Known SLDs of Au ( $4.51 \times 10^{-4} \text{ nm}^{-2}$ ) and  $\text{D}_2\text{O}$  ( $6.30 \times 10^{-4} \text{ nm}^{-2}$ ) were used for analysis. The SLD of dendrimer ( $0.42 \times 10^{-4} \text{ nm}^{-2}$ ) was estimated from the SLDs of elements constituting the dendrimer and molecular volume.<sup>37</sup>

## Results and Discussion

**Hybridization of Au-NPs on Dendrimer LB Films.** The dendrimer Langmuir films at various surface pressures on water subphase were transferred onto TEM grids, and the grids were immersed into the Au-NP suspension for 2 h. The TEM images of Au-NPs on the dendrimer LB films are shown in Figure 2. The Au-NPs were scarcely adsorbed on the TEM grid without the dendrimer LB film (data not shown). On the other hand, on the LB film prepared at 0 mN/m, the Au-NPs in small domains formed a hexagonal lattice with an interparticle distance of approximately 2 nm. This means that a Au-NP is coated by a dendrimer shell of  $\sim 1$  nm thickness. At higher surface pressures, fewer amounts of Au-NPs were adsorbed as disordered small domains on the films. At 40 mN/m, Au-NPs formed lines on the LB film. Despite the fact that the adsorption of Au-NPs was abundant on the dendrimer LB film prepared at 0 mN/m, it was less on the film at high surface pressures. This suggests that the dendrimer at the air/water interface changes its conformation at high surface pressures so as to hide the binding sites of dendrimers.

The binding sites for Au-NPs are amine groups in a dendrimer,<sup>30</sup> which are hydrophilic and face water subphase at 0 mN/m. As the Langmuir film is compressed, the binding sites segregate from the subphase by a conformational change from “face-on” to “edge-on”, as shown in Figure 1. Such a conformational change has been reported for azacrown derivatives substituted by long alkyl chains.<sup>38</sup> Although we previously reported that the aza-C6-PAMAM dendrimer with methyl ester terminals maintained “face-on” conformation on water subphase even at high surface pressures,<sup>30</sup> the enhanced amphiphilicity of the dendrimer with octyl terminals in the present work could stimulate the conformational change.

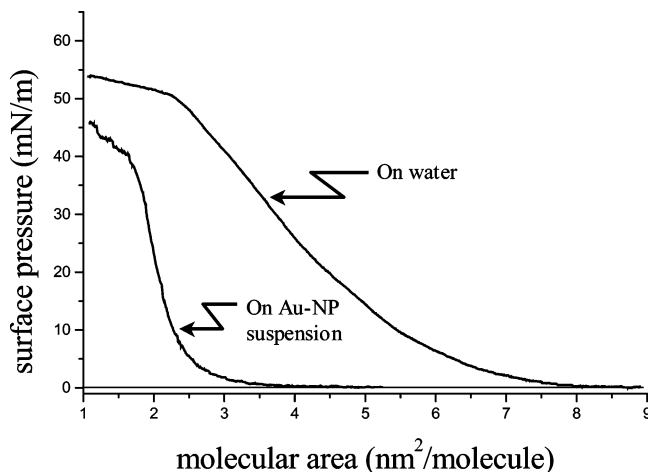


**Figure 3.**  $\pi$ - $A$  isothermal curves of G1.5 aza-C6-PAMAM dendrimer on water and Au-NP suspension subphases.

The  $\pi$ - $A$  isothermal curve of the dendrimer on water subphase is shown in Figure 3. The surface pressure increased gradually from 0 mN/m ( $\sim 8.0 \text{ nm}^2/\text{molecule}$ ) to a collapse pressure ( $\sim 50 \text{ mN/m}$ ,  $2.3 \text{ nm}^2/\text{molecule}$ ). In comparison to the calculated molecular area of a flattened dendrimer structure ( $\sim 28 \text{ nm}^2/\text{molecule}$ ), the observed small molecular area indicates that the hydrophobic terminal groups stand up from the subphase even at 0 mN/m, consistent with the “face-on” model. The hexagonal lattice formation of Au-NPs at 0 mN/m (Figure 2) implies that the dendrimer LB film worked as a template with the ordered structure of Au-NPs. Since the dendrimer in “face-on” conformation occupied the circular surface area of  $\sim 8.0 \text{ nm}^2/\text{molecule}$  at 0 mN/m, the diameter of the circle is  $\sim 3.2 \text{ nm}$ . Thus, Au-NPs adsorb on the hexagonal lattice of dendrimer and can arrange in a hexagonal lattice with a center-to-center distance of  $\sim 6.4 \text{ nm}$ , as illustrated in Figure 2. Then this distance is consistent with the observed composite size (interparticle distance  $\sim 2 \text{ nm}$  + particle size  $\sim 3.9 \text{ nm}$ ) from TEM (Figure 2).

At the collapsing point, the molecular area is about  $2.3 \text{ nm}^2/\text{molecule}$ , which is consistent with the calculated area ( $0.19 \times 12 = 2.3 \text{ nm}^2$ ) for 12 terminal groups in the “face-on” model. However, owing to the bulky structures and limiting configuration of dendron branches, such close packing of terminal groups is unlikely taken. Alternatively, the dendrimer can change its conformation to “edge-on” (Figure 1). Since platelike “edge-on” dendrimers could be packed more compact than corn-like “face-on” dendrimers, this assumption is considered reasonable. In the film with “edge-on” conformation, the binding sites are hidden from the subphase. Thus, the Au-NPs cannot adsorb to the film. The observation (Figure 2) of disordered small domains of Au-NPs on the dendrimer LB film at high surface pressures implies that the binding sites are partly exposed at defects of the film. The lines of Au-NPs observed in the film at 40 mN/m suggest that cracks are formed in the film, and Au-NPs adsorb to the exposed binding sites along the cracks.

**Hybridization of Au-NPs to Dendrimer Langmuir Film.** Hybridization of Au-NPs with dendrimers was examined at the air/Au-NP suspension interface in a Petri dish. From the mass of spread dendrimer and surface area of the subphase, the surface pressure was estimated to be  $\sim 0 \text{ mN/m}$  with the aid of the  $\pi$ - $A$  isothermal curve of dendrimer on Au-NP suspension (Figure 3). As seen in photographs of air/Au-NP suspension interfaces in the Petri dish (Figure 4), when dendrimers were spread, a dark

(37) Mitamura, K.; Imae, T. *Trans. Mater. Res. Soc. Jpn.* **2003**, *28*, 71.

(38) Gidalevitz, D.; Mindyuk, O. Y.; Stetzer, M. R.; Heiney, P. A.; Kurnaz, M. L.; Schwartz, D. K.; Ocko, B. M.; McCauley, J. P.; Smith, A. B. *J. Phys. Chem. B* **1998**, *102*, 6688.

(39) Sui, G.; Mabrouki, M.; Ma, Y.; Micic, M.; Leblanc, R. M. *J. Colloid Interface Sci.* **2002**, *250*, 364.

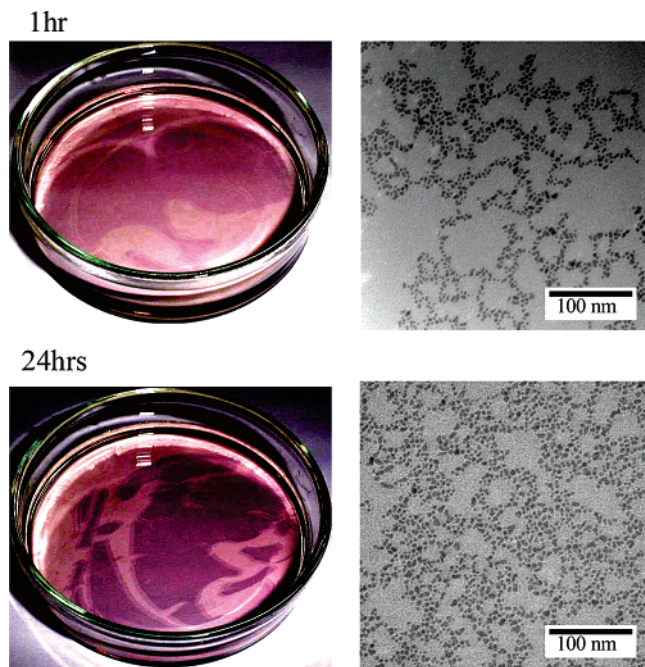


**Figure 4.** Photographs of Langmuir films in Petri dish (left) and TEM images of LB films transferred from the Langmuir films in Petri dish (right).

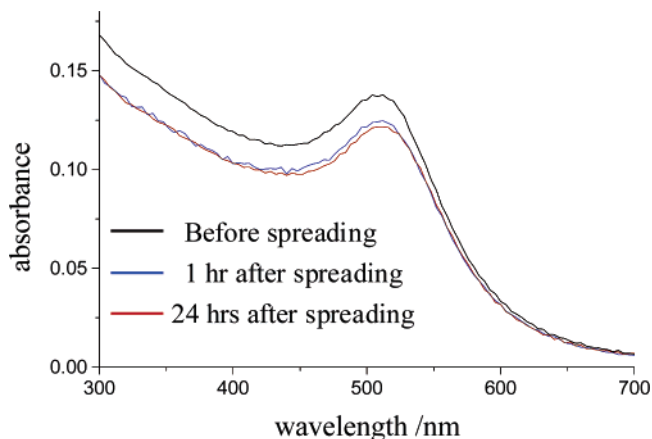


**Figure 5.** UV-vis absorption spectra of Au-NP suspensions before and after spreading of dendrimer.

red fluid film appeared at the interface after 1 h, and the film shrank and became violet and crumbly after 24 h. At the same time, the plasmon band at 510 nm in the UV-vis absorption spectra of the subphase was weakened down to ca.  $\frac{7}{8}$  without position change at 1 h after spread of dendrimer (Figure 5). However, the same intensity was maintained even after being left for more than 1 h. This means that the adsorption was accomplished within 1 h. Incidentally, when the dendrimers were not spread, the colored film did not appear, and the plasmon band of the subphase did not change its intensity. On TEM images of LB films of dendrimer/Au-NP composites, a fractal-like floc texture of dendrimer/Au-NP composites was observed throughout the film after 1 h but only in the shrunk film with high composite density after 24 h. However, the array of Au-NPs was still a monolayer without overlap. The time-dependent condensation of the flocs after the accomplishment of adsorption can result from the attractive interactions, which are van der Waals force between Au-NPs and hydrophobic interaction between terminal alkyl chains in dendrimers surrounding Au-NPs. The terminal octyl groups in dendrimers should provide stronger intermolecular hydrophobic interaction than the methyl ester groups did: When

methyl ester-terminated dendrimer was used for hybridization, nanoparticles were dispersed without fractal-like aggregation.<sup>30</sup>

The number of Au-NPs in the subphase before adsorption can be calculated from the average diameter of spherical Au-NP and the concentration of Au atom in the subphase. Considering that about  $\frac{1}{8}$  of Au-NPs adsorbed onto the dendrimer film, it is evaluated that the number of dendrimer molecules on one Au-NP is  $\sim 14$ . The center-to-center distance ( $\sim 7$  nm) of a dendrimer/Au-NP composite was evaluated from TEM images, although this value was slightly larger than that ( $\sim 6.4$  nm) on a dendrimer LB film (Figure 2), where the order of the Au-NPs was controlled by ordered dendrimer arrangement. Supposing that the dendrimer/Au-NP composite is a sphere, each of the 14 dendrimer molecules can occupy  $\sim 11$  nm<sup>2</sup> of the Au-NP surface. This value is nearly double the occupied molecular area of dendrimer at the air/water interface (Figure 3). Alternatively, volume of 14 dendrimer molecules can be  $\sim 57.4$  nm<sup>3</sup> from molecular formula (C<sub>198</sub>H<sub>390</sub>N<sub>30</sub>O<sub>18</sub>) and density ( $\sim 1.4$  g/cm<sup>3</sup>).<sup>37</sup> This is almost half of the volume ( $\sim 146$  nm<sup>3</sup>) of the dendrimer shell as a sphere. Thus, it is reasonable that the dendrimers occupy only half of the Au-NP surface. If 14 dendrimer molecules share the area occupied by a dendrimer/Au-NP composite at the interface, the apparent molecular area per dendrimer is 2.7 nm<sup>2</sup>/molecule, which is close to the occupied molecular area ( $\sim 2.3$  nm<sup>2</sup>/molecule) of dendrimer on Au-NP suspension subphase (Figure 3). This result also supports the assumption for occupation of dendrimers on the Au-NPs.

To clarify the aggregation of the dendrimer/Au-NP composite and its surface pressure dependency after 1 h adsorption, the hybrid LB films at different surface pressures were observed by TEM (Figure 6). Before compression ( $\sim 0$  mN/m), the film consisted of fractal-like networks of composites, as already observed in Figure 4 (upper panel). At surface pressures of 5 and 20 mN/m, the composites further flocculated to form a condensed monolayer. At 30 mN/m, just below the collapsing surface pressure, the composites formed a uniform film with some defects, and additionally, lined zones of high electron density were observed, indicating that the film started collapsing and the composites were overlapped at the zones. The interparticle distance of Au-NPs scarcely changed at the whole surface pressures up to 30 mN/m.

**Structure of Au-NPs in Dendrimer/Au-NP Composites at Interfaces.** Neutron reflectivity was measured for the dendrimer/Au-NP hybrid film ( $\pi = 5$  mN/m) on the Au-NP suspension in order to confirm the structure of Au-NPs. A decay curve without fringe was observed (Figure 7a). For analysis, two types of models consisting of 8 layers were assumed. In type 1, the dendrimers fully surround the surface of the Au-NP. On the other hand, the dendrimers cover only the upper-half surface of the Au-NP in type 2. Comparing the observed curve with the calculated ones based on the two models, the curve of type 2 was more suitable to the observed reflectivity profile without fringe than that of type 1, as seen in Figure 7a. The depth vs SLD profile calculated from optimum parameters with the type 2 model is shown in Figure 7c, where the depth positions of dendrimer and Au-NP regions on the suspension are also illustrated. It was clarified that 14 dendrimers distributed only on the upper-half surface of a Au-NP at the air/suspension interface, as illustrated in Figure 8a.

Since the thickness ( $\sim 3.5$  nm) of the gold region in the depth-SLD profile is close to the observed diameter of a Au-NP, it was clarified that the Au-NPs formed a monolayer. Meanwhile, the calculated SLD of the Au-NP region was  $1.1 \times 10^{-4}$  nm<sup>2</sup>, which is only  $\sim 24\%$  of the theoretical value for Au. Au-NPs at interface

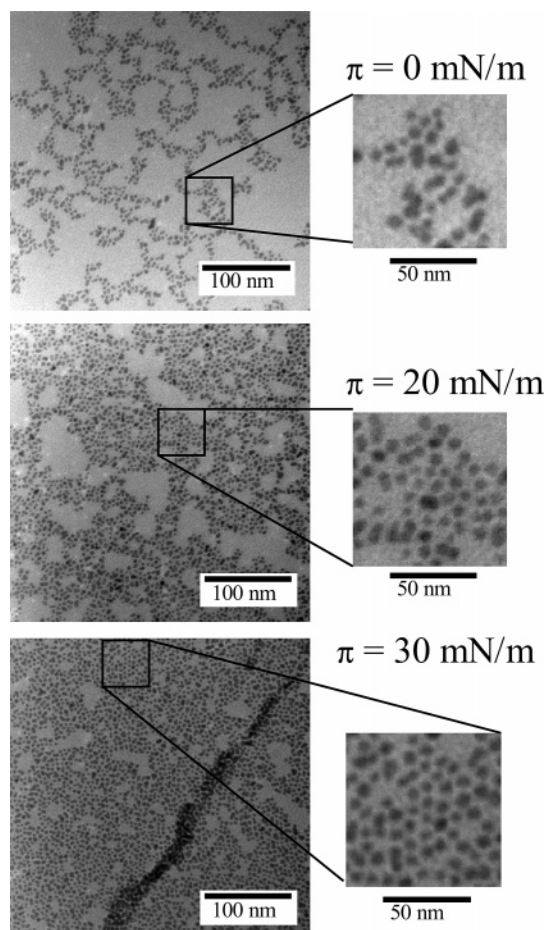


**Figure 6.** TEM images of LB films transferred from the Langmuir films at air/suspension interface at various surface pressures.

should take a hexagonal lattice array with a particle core-to-core distance of  $\sim 7$  nm (as described above), while the diameter of Au-NP was  $\sim 3.9$  nm. Thus, the Au-NP could be in a hexagonal lattice cell with these sizes, as illustrated in Figure 8b. The volume fraction of a Au-NP in the cell is calculated as a volume ratio of a Au-NP sphere to a hexagonal cell, that is,  $31.0/195$  ( $\text{nm}^3/\text{nm}^3$ ) =  $\sim 16\%$ . Thus, contribution of Au-NP to SLD is  $\sim 0.72 \times 10^{-4} \text{ nm}^2$  ( $= 4.51 \times 10^{-4} \times 0.16$ ). On the other hand, in type 2, since half of the rest ( $\sim 84\%$ ) of the cell should be filled with the dendrimer, the contribution of dendrimer to SLD is  $\sim 0.35 \times 10^{-4} \text{ nm}^2$  ( $= \sim (0.42 \times 10^{-4} \times 0.84)/2$ ). Therefore, total SLD should be  $\sim 1.07 \times 10^{-4} \text{ nm}^2$ , which agreed well with the observed SLD.

Although reflectivities at pure  $\text{D}_2\text{O}$  and Au-NP suspension interfaces without dendrimer monolayer were referred, the depth profiles were quite similar to each other but different from that of the dendrimer/Au-NP hybrid film on the Au-NP suspension, as seen in Figure 7c. This means that the Au-NPs are not sheathed at the interface without the dendrimer. In other words, the dendrimer film is necessary for forming a Au-NP monolayer at air/water interface.

For verification of type 2, an X-ray reflectivity measurement was carried out for the dendrimer/Au-NP composite film transferred onto silicon substrate at a surface pressure of 10 mN/m. The resultant X-ray reflectivity is shown in Figure 7b. At the fitting calculation, two models were examined. In model 1, two dendrimer regions were located at the top and bottom of a Au-NP region, instead of a monolayer of Au-NPs fully coated by the dendrimer shells. Model 2 consists of a Au-NP region and a dendrimer region, as modification of a monolayer of Au-NPs

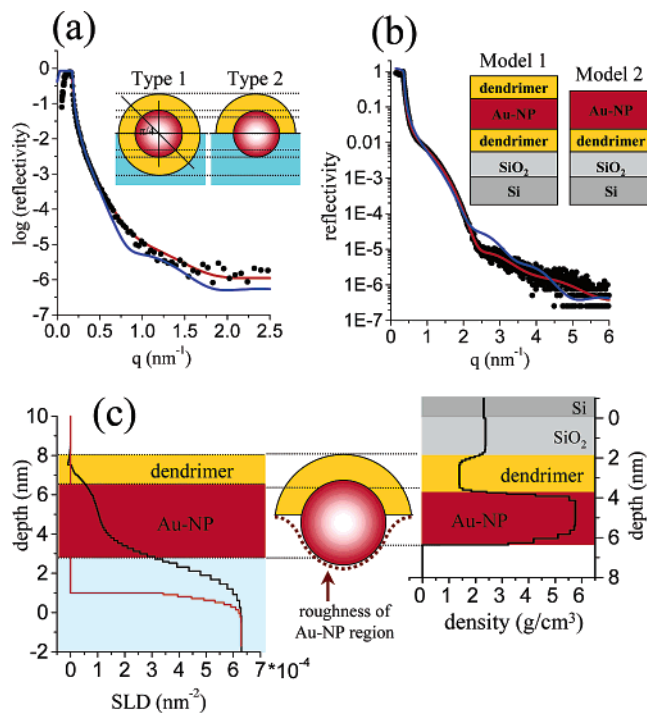


**Figure 7.** Neutron and X-ray reflectivity of the dendrimer/Au-NP hybrid film at air/subphase interface and on silicon substrate, respectively, and their analysis. (a) Neutron reflectivity: observed (closed circle), type 1 based fitting (solid blue line), and type 2 based fitting (solid red line) curves. (b) X-ray reflectivity: observed (closed circle), model 1 based fitting (solid blue line), and model 2 based fitting (solid red line) curves. (c) Left: depth vs SLD profiles of dendrimer/Au-NP hybrid Langmuir film (based on type 2) (black) and  $\text{D}_2\text{O}$  and Au-NP suspension subphases (red). Right: depth vs density profile (based on model 2). Dendrimer and Au-NP regions are illustrated in part c with corresponding model.

half-coated by the dendrimer shells. (These models are alternatives to the models used in neutron reflectivity. Although two models for neutron reflectivity are preferable, those for X-ray reflectivity had to be modified so as to adapt to the computer program.) According to the analytical procedure, the optimum parameters were determined for both models and the calculated curves were compared with the observed one. Model 2 (half-surface-coated model) fitted better than model 1 (whole-surface-coated model). Thus, dendrimer molecules distributed only on the upper side of a Au-NP at air/water interface, since the Langmuir film was transferred by the Langmuir–Schaefer method (Figure 8c).

The density ( $5.8 \text{ g/cm}^3$ ) of the Au-NP region was  $\sim 30\%$  of bulk Au density ( $19.3 \text{ g/cm}^3$ ), as seen from the depth vs density profile (Figure 7c). This value is larger than that ( $\sim 24\%$ ) calculated from the neutron reflectivity, but the thickness ( $\sim 2.5$  nm) of the Au-NP region is thinner than that ( $\sim 3.5$  nm) from neutron reflectivity. This difference is attributed to the virtual layer model for X-ray reflectometry. The Au-NP region was obtained with thickness of 2.5 nm and roughness of 0.7 nm. It is apparent from Figure 7c that the Au-NP surface must be rough, when the type 2 model is applied. Thus, results from X-ray reflectivity are consistent with a transferred monolayer of half-coated dendrimer/Au-NP composites, as schematically illustrated in Figure 8c.

## Conclusions

A monolayer of Au-NP was formed at the air/liquid interface with the aid of a Langmuir film of amphiphilic dendrimer. G1.5 poly(amido amine) dendrimer with an azacrown core, hexylene

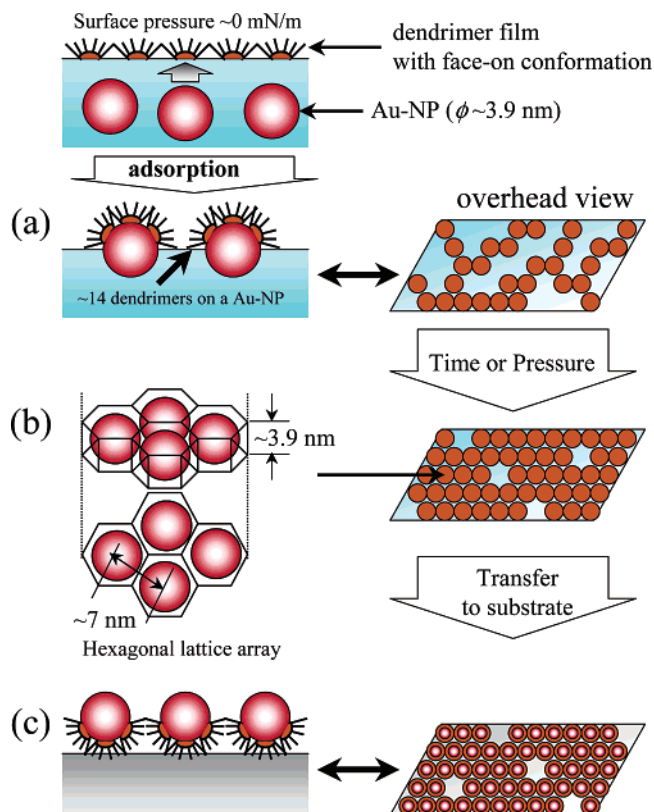


**Figure 8.** Formation of the dendrimer/Au-NP hybrid films at interfaces via hybridization at the air/suspension interface and transfer to the solid substrate.

spacers, and octyl terminals was hybridized with gold nanoparticle (Au-NP) at the interface. Formation of a fractal-like network of flocs at  $\sim 0$  mN/m was clarified from TEM images of hybrid

films. The network was densified with time or compression and became a defect-existing monolayer of Au-NPs. Au-NPs in the monolayer were arranged in hexagonal lattice. Binding of 14 dendrimer molecules on a Au-NP was evaluated from the intensity of a particle plasmon band. Then, referring the occupied molecular area and the hexagonal lattice arrangement, the dendrimers were assumed to occupy only the half surface area of the Au-NP. Moreover, it was confirmed from neutron and X-ray reflectivities that the dendrimers were localized only on the upper-half surface of Au-NP at the air/liquid interface.

In the formation of the dendrimer/Au-NP composite, the flexible hexylene spacers allowed the dendrimer conformation to vary, and the exposed azacrown core acted as an effective binding site for metal nanoparticle. For the fabrication of the monolayer, the octyl terminals stimulated flocculation of the dendrimer/Au-NP composites by their hydrophobic interaction, and the van der Waals attraction between composites reinforced the flocculation. The dendrimer template utilized in the present work in order to fabricate a nanoparticle monolayer is useful for many applications, because the obtained films possess hexagonal lattice ordering of nanoparticles with half surfaces as anchors on the dendrimer template and bare half surfaces as functional sites. Additionally, the dendrimer shell also could be functionalized for advanced applications.

**Acknowledgment.** M.U. thanks the 21st Century COE Program (No.14 COEB01-00) of Nagoya University for the financial support of a research assistant fellowship. The authors are thankful to Dr. O. S. Yemul for his technical assistance with the synthesis of dendrimers. The present work was partly supported by the Grant-in-Aid for Scientific Research (B) (15350067) from Ministry of Education, Culture, Sports, Science and Technology (MEXT), Japan.

LA053202N